MOLECULAR AND CELLULAR BIOLOGY, Oct. 2005, p. 9151–9164 Vol. 25, No. 20
0270-7306/05/$08.00+0 doi:10.1128/MCB.25.20.9151–9164.2005

Germ Line Transcripts Are Processed by a Dicer-Like Protein That Is Essential for Developmentally Programmed Genome Rearrangements of *Tetrahymena thermophila*

Colin D. Malone,† Alissa M. Anderson,† Jason A. Motl,† Charles H. Rexer, and Douglas L. Chalker*

Biology Department, Washington University, St. Louis, Missouri 63130

Received 1 April 2005/Returned for modification 4 May 2005/Accepted 19 July 2005

Abundant ~28-nucleotide RNAs that are thought to direct histone H3 lysine 9 (H3K9) methylation and promote the elimination of nearly 15 Mbp of DNA from the developing somatic genome are generated during *Tetrahymena thermophila* conjugation. To identify the protein(s) that generates these small RNAs, we studied three Dicer-related genes encoded within the *Tetrahymena* genome, two that contain both RNase III and RNA helicase motifs, Dicer 1 (DCR1) and DCR2, and a third that lacks the helicase domain, Dicer-like 1 (DCL1). *DCL1* is expressed upon the initiation of conjugation, and the protein localizes to meiotic micronuclei when bidirectional germ line transcription occurs and small RNAs begin to accumulate. Cells in which we disrupted the *DCL1* gene (Δ*DCL1*) grew normally and initiated conjugation as wild-type cells but arrested near the end of development and eventually died, unable to resume vegetative growth. These Δ*DCL1* cells failed to generate the abundant small RNAs but instead accumulated germ line-limited transcripts. Together, our findings demonstrate that these transcripts are the precursors of the small RNAs and that *DCL1* performs RNA processing within the micronucleus. Postconjugation Δ*DCL1* cells die without eliminating the germ line-limited DNA sequences from their newly formed somatic macronuclei, a result that shows that this Dicer-related gene is required for programmed DNA rearrangements. Surprisingly, Δ*DCL1* cells were not deficient in overall H3K9 methylation, but this modification was not enriched on germ line-limited sequences as it is in wild-type cells, which clearly demonstrates that these small RNAs are essential for its targeting to specific loci.

RNA interference (RNAi) describes an array of related mechanisms involved in diverse biological processes including defense against RNA viruses, specification of centromeric heterochromatin structure, and developmental control of gene expression (reviewed in reference 25). These mechanisms share the use of small RNAs to target specific effector protein complexes to homologous sequences via base-pairing interactions. The use of small, homologous RNAs as specificity factors imparts tremendous flexibility of targets on a single protein complex. These targeting RNAs are generated by RNase III enzymes, collectively called Dicer ribonucleases, that cleave longer, double-stranded RNA (dsRNA) into ~20- to 26-nucleotide (nt) species that are incorporated into the effector complexes (3, 24, 27, 30; reviewed in reference 6). The genomes of many eukaryotes encode multiple Dicer-related proteins, and the specific Dicer used to generate the small RNAs can determine the downstream pathway that they enter. For instance, in *Arabidopsis thaliana*, the Dicer-like 3 (Dcl3) gene product is required to produce endogenous short interfering RNAs (siRNAs), *A. thaliana* Dcl2 is necessary for accumulation of siRNAs in response to RNA virus infections, and *A. thaliana Dcl1* is necessary to generate micro-RNAs (miRNAs) involved in the control of flower development (31, 53). Similarly, the *Drosophila melanogaster* Dcr-1 and Dcr-2 genes exhibit distinct roles in siRNA and miRNA regulatory pathways (33). Nevertheless, the diversification of these related pathways remains understood in only the most general ways.

Developmentally programmed genome reorganization of the ciliate *Tetrahymena thermophila* is one of the processes that is directed by homologous, small RNAs (reviewed in reference 43). Ciliates, including *Tetrahymena*, are single-celled organisms that exhibit nuclear dualism, possessing both germ line and somatic genomes that are harbored within distinct nuclei, called micro- and macronuclei, respectively (46). Massive DNA rearrangements are part of the differentiation of somatic macronuclei from germ line micronuclei, which retains the organism's genome intact for future propagation (55). The developmental program during which this nuclear differentiation occurs is initiated by conjugation. Within the first hours of conjugation, the germ line micronucleus within each mating partner undergoes meiosis to produce four haploid pronuclei, one of which is then selected to replicate its DNA and divide to generate one stationary and one migratory gametic nucleus. Nuclear exchange of the migratory nucleus is followed by karyogamy with the partner's stationary nucleus, resulting in the formation of a diploid, zygotic nucleus in each cell. This nucleus proceeds to divide twice, generating the progenitors of the new germ line and somatic nuclei of the progeny from the mating. The parental somatic nuclei begin to degenerate upon formation of these new nuclei.

During nuclear differentiation, the germ line-derived chromosomes within the developing somatic nucleus are broken at 200 to 300 sites. This chromosome breakage is coupled to new

* Corresponding author. Mailing address: Biology Department, Washington University, Campus Box 1137, St. Louis, MO 63130. Phone: (314) 935-8838. Fax: (314) 935-4432. E-mail: dchalker@biology2.wustl.edu.

† C.D.M., A.M.A., and J.A.M. contributed equally.

telomere addition. In addition, ~15 Mbp of DNA is eliminated by specific DNA rearrangements of an estimated 6,000 loci (the DNA segments excised are often called internal eliminated sequences [IESs]). These germ line-limited DNA segments range in size from a few hundred base pairs to more than 20 kbp and are comprised of both unique sequences as well as repetitive elements. While flanking regulatory sequences that demarcate the boundaries of specific deletion events have been identified (8, 17, 21, 22, 45), identification of any consensus sequences that are required to promote these DNA rearrangements has remained elusive. The heterogeneity of the sequences eliminated, together with the lack of a defined consensus sequence, has provided a challenge in describing a simple model for the control of this process.

Recent studies have revealed that *Tetrahymena* DNA rearrangements are guided by an RNAi-related mechanism. Abundant small (28- to 30-nt) RNAs that are enriched in germ line-limited sequences are produced early in development (9, 40). These are suspected to result from the processing of bidirectional transcripts produced in the germ line micronucleus that begin accumulating at the earliest stages of conjugation (11). The finding that the Argonaute homologue Twi1 protein (Twi1p) is required for the accumulation of these small RNAs (named scan RNAs) and for DNA rearrangement provided the first direct link between genome reorganization and RNAi (40). Yao et al. (56) demonstrated that RNA guides DNA rearrangements by injecting dsRNA corresponding to macronuclear regions into conjugating cells and documenting the elimination of the homologous DNA sequence that would normally be retained. Furthermore, it appears that these small RNAs target methylation of lysine 9 of histone H3 (H3K9) (H3K9me) to homologous sequences within the developing somatic macronuclei shortly after they are formed, and this modification is required for DNA rearrangement (34, 50). This modification is presumed to mark specific sequences for elimination by recruiting the machinery that excises the germ line-limited DNA and rejoins the flanking sequence that is retained in the mature somatic genome. This pathway of DNA rearrangement possesses the hallmarks of heterochromatin formation in other eukaryotes, thus making this process an intriguing model with which to study RNAi-directed, genome-wide targeting of this chromatin modification.

Further evidence that DNA rearrangement is controlled by a homology-based recognition system is the observation that germ line-limited sequences introduced into the parental somatic macronucleus block the efficient elimination of their cognate sequences from the developing macronucleus during subsequent nuclear differentiation (10). This sequence-specific inhibition applies even to a cell's wild-type conjugation partner by a method that does not require genetic exchange, a finding that supports the action of homologous RNAs as mediators of this regulation (9). Similar homology-based regulation of DNA rearrangement has been described in the ciliate *Paramecium tetraurelia* (13, 14). Small (23-nt) RNAs have also been implicated in these events (20), indicating that the rearrangement processes of these different ciliates are mechanistically related. The interplay between the germ line and somatic genomes suggests that DNA rearrangement in ciliates is a mechanism of genome surveillance that provides a means to remove foreign sequences from the transcriptionally active genome during development, thus limiting their spread. In support of this, transgenes introduced into the germ line genome can be eliminated from newly formed somatic macronuclei in a process that looks remarkably similar to the process of endogenous genome rearrangements (35, 56).

The bidirectional germ line transcription that occurs early in conjugation provides a source RNA that could be compared between the germ line and somatic genomes and later target sequences found exclusively in the germ line for elimination by the DNA rearrangement machinery. To demonstrate a clear connection between germ line transcription, small RNAs, and DNA rearrangement, we searched the *Tetrahymena* draft genome sequence for candidate Dicer RNase homologues that might encode the enzyme(s) that generates the small RNAs that target elimination. We show that one of three putative Dicer-related genes, *DCL1*, is localized to meiotic micronuclei and is required to process germ line transcripts into these 28- to 30-nt RNAs. Strains lacking *DCL1* are unable to complete development and fail to eliminate germ line-limited sequences from the developing somatic genome. The two other Dicer-related genes, each of which exhibits expression patterns distinct from that of *DCL1*, are not redundant to DCL1; thus, it would appear that even single-celled organisms can differentiate RNAi pathways by the specialization of Dicer function.

MATERIALS AND METHODS

Stocks and growth conditions. *Tetrahymena* cells were grown and maintained in 1× SPP at 30°C (44a). Cells were prepared for mating by washing cells from growth medium into 10 mM Tris-HCl (pH 7.4) and incubation overnight prior to mixing to initiate conjugation. Wild-type, inbred *Tetrahymena thermophila* strains (obtained from Peter Bruns, Cornell University) CU428 (Mpr/Mpr [VII, mp-s]), B2086 (II), and CU427 (Chx/Chx [VI, cy-s]) were used for all expression studies, biolistic transformations, and subsequent analyses. The micronucleus-defective "star" strains B*VI and B*VII were used to convert heterozygous Δ*DCL1* lines to micronuclear homozygosity by genomic exclusion crosses. Δ*TWI1* germ line/somatic knockout lines WG4 and 12-1A were provided by K. Mochizuki (University of Rochester, Rochester, NY).

Sequence identification. Three Dicer homologues were identified by BLAST search of the *Tetrahymena* genome (http://tigrblast.tigr.org/er-blast/index.cgi?project=ttg Assembly 2 [accessed November 2003]) using human Dicer1 (GenBank accession number gi29294651), *Drosophila melanogaster* CG6203-PA (accession number gi19922726), and the *Arabidopsis thaliana* endonuclease Dicer homologue (CARPEL FACTORY protein [accession number gi34922211]). The extents of the coding regions were initially predicted by visual inspection for higher GC content and proper intron/exon splice sites and are as follows: *DCR1*, positions 59218 to 66953 of scaffold CH445757 (accession number gi62422189); *DCR2*, positions 110642 to 117676 of scaffold CH445577 (accession number gi62422369); and *DCL1*, positions 808498 to 804612 of scaffold CH445618 (accession number gi62422328). Current sequence identification numbers from the *Tetrahymena* genome database (http://www.ciliate.org) are as follows: Dcr1p, T000006591; Dcr2p, T000006592; and Dcl1p, T000006590. Partial or full cDNA sequences were deposited in GenBank during the course of this work (gi50897087, gi50897083, and gi50897085) (42). Conserved domains were identified using the Pfam Protein Family Database (http://pfam.wustl.edu/).

Generation of DCL1 knockouts. Upstream *DCL1* sequences plus the first 189 codons of exon 1 (scaffold positions 807496 to 809192) and downstream sequence spanning codons 636 to 1254 including the lone intron (scaffold positions 804682 to 806496) were PCR amplified from genomic DNA and cloned individually into pCR2.1 using the TOPO TA cloning kit (Invitrogen). ApaI-XhoI or BamHI-NotI recognition sites were introduced into the ends of upstream and downstream oligonucleotide primer sets (Table 1), respectively, to facilitate insertion of the fragments into pMNBL flanking the metallothionein 1 (MTT1) promoter-driven *neo3* cassette (*MTT1*-neo) (48). The resulting *DCL1* knockout construct substituted 1.3 kbp of the coding sequence with the *neo3* cassette, effectively removing amino acids 190 to 638 from DCL1. This construct was linearized by digestion with ApaI and NotI and introduced into conjugating B2086 and CU428 cells between 2 and 3 h after mixing using a PDS-1000/He particle bombardment

TABLE 1. Oligonucleotides used in course of this study

Purpose and name	Sequence (5′–3′)
To amplify *DCL1* sequence for generation of knockout construct	
#1358-DCL1-10044B	ATAGGATCCAGTCTTGCTTACAAAAAGAC
#1359-DCL1-11863Nr	ATAGCGGCCGCATCTTAGAAGGCTTTTTTTTCAGC
#1429-DCL1-7349A	ATAGGGCCCACACCTTTATATATCATTTCC
#1430-DCL1-8616Xr	ATACTCGAGGATGATAGGCTTATAGTAG
To screen knockouts during assortment to complete replacement	
#1403-DCL1-9934	ATACCATCAATTTAATCGCCG
#1402-DCL1-10206r	TCTCTAACAATCATGACATCT
#1399-neo3-3351	TCGCCTTCTTGACGAGTTCT
To verify expression knockouts via RT-PCR	
#1471-DCL1-806111	AGGAATTTCAGCGTTTAGAAACGGTC
#1470-DCL1-805866r	CATAAAAGCACCCAACAACTG
#1413-ATU1-1997	TGCTCGATAACGAAGCCATCT
#1412-ATU1-2391r	GTGGCAATAGAAGCGTTGACA
To clone *DCL1* coding sequence for fusion to GFP	
#1445-DCL1-8048X	ATACTCGAGATGAGAAACAAACCTAAAGTTA
#1394-DCL1-11862Ar	ATAGGGCCCATCTTAGAAGGCTTTTTTTTCAGC
To assess enrichment of sequences after chromatin immunoprecipitation	
#1228-BTU-39f	GTACCACCACCGAGGGAGTGGGTG
#1229-BTU1-404r	TAACCAAATTGGTGCTAAGTTCTG
#1240-R-661f	ATGAGGTAAATTGAGGAGGGGAGC
#1241-R-834r	CATGTTTAGCTTGATAATTACTTTTCC
#1242-M-1418f	AAATTGAATAAGGAGACCAGCCTCTC
#1243-M-1635r	TATCAGTTCTCATCAAGTTGTAATGC
#1596-MAC-IR-676r	AGACCCGTAGAAAGCTAACTCCC
#1597-MAC-IR-902r	GAATGAAGGAGACATCGTCTAATA

system (Bio-Rad) as previously described (4, 7). Cells were allowed to complete conjugation in 10 mM Tris overnight before transfer to growth medium. Transformants were selected in 1× SPP containing 1.0 μg/ml $CdCl_2$ and 80 μg/ml paromomycin sulfate (PM) (Sigma) after preinduction of the *neo3* cassette in 1× SPP containing 0.5 μg/ml $CdCl_2$ for 5 to 6 hours at 30°C. Transformants were assessed for disruption of the germ line *DCL1* locus by crossing mature lines with CU427 and testing the cycloheximide-resistant cells (true progeny) for propagation of the *neo3* cassette allowing growth in medium containing $CdCl_2$ and PM (5). The heterozygous germ line knockouts were serially transferred (i.e., subcloned) into increasing concentrations of PM (from a starting concentration of 80 μg/ml to a final concentration of 350 μg/ml; the $CdCl_2$ concentration remained at 1 μg/ml), allowing for random assortment of macronuclear chromosomes until all wild-type alleles had been replaced with a disrupted copy. This assortment to completion of the knockout was monitored by PCR screening (primers are listed in Table 1) of crude cell lysates (9). Lines with complete macronuclear replacement of wild-type *DCL1* were converted to micronuclear homozygosity by crossing with star strain B*VI or B*VII to induce genomic exclusion. Exconjugates from these matings were screened for growth in $CdCl_2$/PM-containing medium to identify the transformant-derived lines and then crossed with CU427 to verify lines that were homozygous for the mutant allele (which produced 100% cycloheximide-, $CdCl_2$-, and PM-resistant progeny).

Southern blot analysis. Total genomic DNA was isolated from vegetative or conjugating cells by gentle lysis using the Promega genomic DNA isolation kit. DNA was digested with appropriate restriction enzymes before standard fractionation on agarose–1× Tris-borate-EDTA gels and subsequent transfer to nylon membranes (Osmonics) by downward capillary blotting in 0.5 M NaOH–1.5 M NaCl. Membranes were hybridized at 65°C with radiolabeled probes in 6× SSC (1× SSC is 0.15 M NaCl plus 0.015 M sodium citrate)–0.1 M Tris (pH 7.5)–0.5% sodium dodecyl sulfate (SDS)–2× Denhardt's solution for >16 h and then washed at 65°C in 1× SSC–0.5% SDS to remove nonspecific hybridization. All probes were radiolabeled with [α-^{32}P]dATP, random hexamers, and DNA polymerase I (Klenow fragment). Hybridization was visualized by autoradiography.

To examine the *DCL1* locus in knockout lines before and after genomic exclusion, isolated genomic DNA was digested with HindIII, fractionated by electrophoresis, and hybridized to a radiolabeled fragment corresponding a ~1-kbp region within exon 2. To assess failure of DNA rearrangement or chromosome breakage, total genomic DNA isolated from wild-type or Δ*DCL1* cells after ≥30 h of mating was digested with EcoRI, fractionated, and probed with the following radiolabeled fragments: a 1.9-kbp fragment from pDLCM3 detecting the M-element region (10), a 0.38-kbp fragment upstream of the CaM gene detecting CaM deletion element rearrangement (10, 29), or HhaI fragments B and C of Tt2512 germ line-specific sequence (11, 54). Chromosome breakage was assessed using a 0.8-kbp probe fragment that spans the EcoRI site at position 335013 of chromosomal scaffold CH445662 (GenBank accession number gi62422284). Hybridization was measured using a Personal FX PhosphorImager (Bio-Rad). Membranes were stripped and reprobed with an alpha-tubulin (*ATU1*) probe (11) under the same conditions as described above and quantified as a normalization control. *ATU1* hybridization to DNA from Δ*DCL1* and the wild type was used to measure the relative loading of each lane, and the average hybridization of two Δ*DCL1* samples was arbitrarily set as 1. This factor was used to normalize the quantification of the relative intensities between different samples.

RNA analysis. RNA was isolated from *Tetrahymena* by RNAsol extraction (15). Northern blot analysis was performed as described previously by Ausubel et al. (2). Small RNAs were fractionated on 15% polyacrylamide–urea–1× Tris-borate-EDTA gels, and larger RNAs were fractionated on 1.2% agarose–1× MOPS (morpholinepropanesulfonic acid)–1% formaldehyde gels as previously described (9). Random-primer-labeled *DCR1* and *DCR2* probes were 686-bp and 902-bp fragments corresponding to sequences between scaffold positions 66282 and 66968 of CH445757and positions 116071 and 116973 of CH445577, respectively. Plus- and minus-strand M-element riboprobes were synthesized from pMint7 and pMint2 as previously described (11). *ACT1* and *PDD1* coding region probes (11) were used for control hybridizations.

Reverse transcription-PCR (RT-PCR) was used to examine *DCL1* expression in vegetative cells and confirm its loss in knockout cells. Total RNA (4 μg) isolated at 2 and 4 h of mating from Δ*DCL1* (subclone 18.6) crossed with Δ*DCL1* (subclone 42.4) or wild-type cells was treated with DNase I for 30 min at 37°C, followed by inactivation by addition of EGTA (pH 8.0) to 2 mM and incubation at 65°C for 10 min. Random hexamers were used to prime reverse transcription of 2 μg of the treated RNA with SuperScript II reverse transcriptase (Invitrogen) according to the supplier's instructions. cDNA generated from 200 ng of starting RNA (equivalent to RNA from ~1,000 cells) was used in 34 to 42 cycles of PCR (annealing temperature of 50°C) using primers designed to amplify the *DCL1*

intron-containing region as a 245-bp genomic or 189-bp cDNA fragment (scaffold positions 805866 to 806111) or in 28 cycles (58°C annealing temperature) with *ATU1* primers (Table 1). To quantify the sensitivity of our RT-PCR reactions, 10-fold dilutions (10 pg to 1 fg [1 fg = ~1,000 molecules]) of a 1.8-kb in vitro-transcribed RNA corresponding to the same *DCL1* downstream region in our knockout construct were added to the 2 μg of cellular RNA prior to reverse transcription. PCR products were fractionated on agarose gels and visualized by ethidium bromide staining.

Monitoring of conjugation. Conjugating wild-type or Δ*DCL1* cells were fixed in Schaudin's fixative (2 parts $HgCl_2$ and 1 part 95% ethanol) at 2-h intervals after cells were mixed to initiate mating (52). DNA was then stained with 4′,6′-diamidino-2-phenylindole (DAPI), nuclear configurations were visualized using a Nikon E600 fluorescent microscope, and images were compared to those described previously by Martindale et al. (38) to determine the stage of development.

Localization of *DCL1*. An amino-terminal fusion of green fluorescent protein (GFP) to *DCL1* was created by PCR amplifying the entire coding sequence of *DCL1* from *Tetrahymena* genomic DNA. An XhoI site was added immediately preceding the ATG start codon, and an ApaI site was added downstream of the stop codon. This fragment was inserted in frame and downstream of GFP into the XhoI and ApaI sites within pIGF-1. This plasmid contains the S65T GFP variant expressed from a 1.2-kbp fragment of the MTT1 promoter all inserted into the NotI site of a pD5H8 rRNA gene vector derivative (22) allowing for autonomous replication. Either pIGF-1 or this GFP-*DCL1* fusion vector was introduced into wild-type cells (B2086 × CU428) or germ line *DCL1* knockouts (BVI $DCL1^{+}$ [$DCL1^{-}/DCL1^{-}$] × BVII $DCL1^{+}$ [$DCL1^{-}/DCL1^{-}$]) by conjugative electroporation (19). Mature transformants were starved overnight in 10 mM Tris and mixed to initiate mating. $CdCl_2$ was added to a final concentration of 0.08 to 0.1 μg/ml to induce expression of the fusion protein. Live cells were harvested 2 to 5 h after mixing, DAPI was added to between 1 and 5 μg/ml, and cells were suspended on glass slides in 2% methyl cellulose. GFP and DAPI fluorescence was visualized by epifluorescence microscopy. Images were captured using a Qimaging RetigaEX charge-coupled-device camera (Burnaby, British Columbia, Canada) and Openlab software (Improvision).

Immunoblotting and chromatin immunoprecipitation. Immunoblot analysis was done as previously described (37). B2086 × CU428, Δ*DCL1* × Δ*DCL1*, and Δ*TWI1* × Δ*TWI1* mating cells (2×10^5 cells/ml of each) were harvested at 7.5 h, 9 h, and 10.5 h after mixing of cells and boiled in lysis buffer prior to separation of proteins on 12% SDS-polyacrylamide gels. Proteins were transferred onto nitrocellulose membranes and incubated with modification-specific antibodies (Upstate Biotechnologies, NY). Antibodies were diluted as follows: anti-H3K9me2 (dimethyl), 1:2,000; or anti-H3K4me3 (trimethyl), 1:5,000. Immunoreactivity was detected using a West Pico kit (Pierce) and autoradiography.

Tetrahymena cells were crossed and prepared for chromatin immunoprecipitation with anti-H3K9me2 (dimethyl) antibodies 9 h into conjugation as described previously (50). After recovery of chromatin/antibody complexes using protein A-Sepharose, DNA was extracted using phenol-chloroform (1:1), and 30 ng was used as a template in PCR with primers (Table 1) specific for either the M element, the R element, or the intervening macronuclear retained region (50). PCR products were resolved on a 1.6% agarose gel and stained with 0.5 μg/ml ethidium bromide. Fluorescence intensities of each were quantified using 1D Image Analysis software (Kodak). Primers amplifying the *BTU1* locus were included in each reaction to generate a quantification standard.

RESULTS

The *Tetrahymena* genome encodes three Dicer-like proteins. To further characterize the relationship between germ line transcription, small RNAs, and DNA rearrangement, we searched the *Tetrahymena* genome for Dicer RNase homologues and found three putative Dicer-related coding sequences (Fig. 1). Two of these contain conserved RNA helicase and RNase III domains characteristic of previously described Dicer homologues (reviewed in reference 6); the third lacks the helicase domain but contains two RNase III domains as well as a dsRNA binding domain. While this work was in progress, partial or full cDNA sequences of these genes were deposited in GenBank (accession numbers are in Materials and Methods), and we have adopted the given names Dicer-1 (*DCR1*) and *DCR2* and Dicer-like-1 (*DCL1*), respectively, for our three identified candidates.

The abundant, small (~28-nt) RNAs that likely guide the extensive DNA rearrangements in developing somatic macronuclei are generated early in *Tetrahymena* conjugation (9, 40, 41). To determine whether any of these Dicer-related genes are particularly good candidates to generate these RNA species, we examined the expression of each, anticipating that the expression of one or more may be conjugation specific. *DCR1* and *DCR2* were observed to be expressed at low levels during all life cycle stages as evidenced by ~7-kb and ~6-kb transcripts, respectively, on Northern blots (Fig. 1D and E). *DCR1* appears to be expressed at slightly elevated levels by 6 h of conjugation, whereas *DCR2* appears to be expressed at its highest levels during vegetative growth. In contrast, *DCL1* expression was not detected by Northern blot in vegetative or starved cells (Fig. 1B). We also performed quantitative RT-PCR for which we should detect even one *DCL1* transcript per cell and verified a lack of appreciable expression in growing cells (Fig. 1C), although we did observe some low-level expression in starved cells (data not shown). In contrast, *DCL1* transcription was rapidly induced within the first 2 h of conjugation. Steady-state levels decreased rapidly between 4 and 6 h until accumulation resumed by 8 h of conjugation. The early high-level expression coincides with the initial accumulation of the development-specific small RNAs by 2 h after mixing of cells (40; also see Fig. 5), thus making the *DCL1*-encoded protein (Dcl1p) an attractive candidate to be involved in their generation.

***DCL1* is required for completion of development.** To determine whether this Dicer-related protein is necessary for the production of these small RNAs, we disrupted the *DCL1* gene in both the macronucleus and micronucleus by homology-directed gene replacement (Fig. 2A). We achieved this by introducing a *DCL1* knockout construct (Fig. 2B) into wild-type strains that directed replacement of 1.3 kbp (encoding 448 amino acids) of the *DCL1* gene with the *neo3* selectable cassette (48) that confers resistance to the drug PM. The initial transformants selected had, on average, half of the somatic *DCL1* gene copies disrupted within the polyploid macronucleus. These lines were subcloned successively into medium containing increasingly higher doses of PM that, due to random segregation (assortment) of macronuclear chromosomes, allowed us to generate lines for which all somatic copies of the *DCL1* gene were replaced with the mutant allele. This macronuclear assortment was assessed by PCR (not shown) and by Southern blot analysis (Fig. 2B) to verify complete loss of the wild-type *DCL1* gene copies except those remaining in the germ line micronucleus. We also verified the disruption of germ line copies of the *DCL1* gene within the micronuclei of these strains using genetic crosses and phenotypic analyses described in Materials and Methods. These initial lines were heterozygous [Fig. 2B, Δ*DCL1* (*n3*/+)] for the knockout allele and were converted to micronuclear homozygosity via genomic exclusion by crossing each line to micronucleus-defective "star" strain B*VI or B*VII. The resulting abortive conjugation proceeds through meiosis and the generation of four haploid (gametic) micronuclear products in the knockout lines, one of which is selected to regenerate into a diploid micronucleus due to the failure of this mating partner to receive a

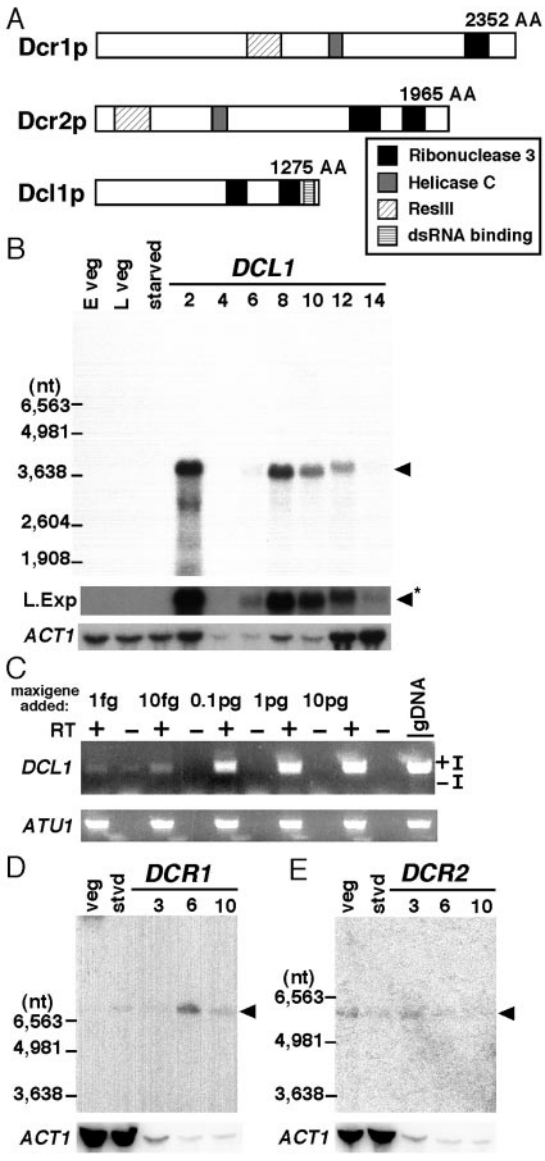

FIG. 1. *Tetrahymena thermophila* encodes three Dicer-like proteins. (A) Total predicted protein length from the *Tetrahymena* genome project is indicated at the right end of each schematic (see Materials and Methods for the locations of each within chromosomal scaffolds). Conserved domains identified by Pfam are indicated by the shaded or hatched boxes (see key). AA, amino acids; dsRNA, small RNA. (B, D, and E) Northern blot analysis was used to examine the expression of Dicer homologues at different life cycle stages. "E veg" refers to early-log-phase vegetative growth, and "L veg" refers to late-log/early-stationary-phase growth. The numbers above each lane denote the hour of mating when RNA was isolated. Arrowheads indicate transcript hybridization. The migration of RNA size markers (Promega) is presented on the left. (B) For *DCL1* expression, a 1-day autoradiogram exposure is shown above a 3-day exposure (L.exp) (arrow with asterisk) that is used to reveal low-level expression at 6 h of conjugation and to highlight the absence of expression in vegetative cells. (C) RT-PCR analysis of RNA isolated from vegetative CU428 cells. The indicated amount of an in vitro-transcribed RNA was added to each 2-μg sample prior to reverse transcription to determine the sensitivity of the assay (1 fg = ~1,000 transcripts). One-tenth (200-ng equivalents) was used in each PCR. *ATU1* amplification was used to confirm cDNA synthesis. gDNA, genomic DNA. (D and E) *DCR1* and *DCR2* expression, respectively, was detected by 5-day exposure of blots to autoradiograph film. To compare loading between samples, each blot was stripped and rehybridized with an actin probe to reveal *ACT1* expression, which is constitutive in vegetative (veg) and starved (stvd) cells but is initially down-regulated early during conjugation before returning to the vegetative level late in development (11 to 12 h).

donor gametic nucleus from the star strain. The cell lines that are now homozygous [Fig. 2B, Δ*DCL1* (*n3*/*n3*)] for the knockout allele in their micronuclei were identified by PCR and verified by genetic crosses with wild-type cells that resulted in 100% propagation of the PM-resistant phenotype to their progeny (data not shown).

Tetrahymena lines lacking all copies of *DCL1* (Δ*DCL1*) exhibited vegetative growth typical of wild-type strains, indicating that this gene is dispensable. This result was not surprising to us, as we could not detect *DCL1* expression in vegetatively growing cells (Fig. 1B). We also generated somatic (macronuclear) knockouts of *DCR1* and *DCR2* (D. L. Chalker, unpublished data). Complete, somatic *DCR1* knockouts exhibited no obvious growth defects, and thus, this gene also appeared to be nonessential. In contrast, after multiple rounds of subcloning, we were unable identify *DCR2* knockout-transformed lines that had reached complete replacement of the wild-type gene with the disrupted allele, a result that suggests that this gene is essential for vegetative growth. These findings indicate that the different RNase III proteins of *Tetrahymena* are not completely overlapping in function.

As *DCL1* expression is induced during conjugation, we crossed two Δ*DCL1* lines to examine the effect of its disruption on development. We verified the loss of *DCL1* expression in these crosses by RT-PCR using oligonucleotide primers that would have detected even low-level transcription of the large carboxy-terminal region remaining in our knockout strains downstream of the *neo3* cassette (Fig. 3A and data not shown). The progression of these mutant cells through conjugation was compared to that of wild-type cells by harvesting cells at 2-h intervals and staining with DAPI to visualize the nuclear configurations that are diagnostic of particular stages of development (Fig. 3B) (38). Δ*DCL1* mating pairs were able to complete most stages of conjugation, although their overall progression was slightly slower than that of wild-type pairs (an observation that was more apparent in some crosses than others but is further evidenced in the crosses shown by the somewhat delayed decrease in *ACT1* expression and accumulation of *PDD1* transcripts [see Fig. 4]). The most dramatic difference observed was that Δ*DCL1* cells failed to eliminate one of the two progenitors of the new micronucleus (Fig. 3C). This corresponds to the last step of conjugation just prior to the return to vegetative growth. This finding suggested that the loss of *DCL1* results in a developmental arrest phenotype. These cells do not appear to fully amplify the genome in the developing macronuclei, as the fluorescence intensity of these nuclei relative to the micronuclei in the same cell upon DAPI staining is lower overall when compared to that of wild-type cells (Fig. 3C and data not shown).

To confirm that Δ*DCL1* cells had arrested late in development, we isolated individual mating pairs of wild-type and Δ*DCL1* cells into separate drops of growth medium and compared their fates. Whereas most wild-type pairs had resumed

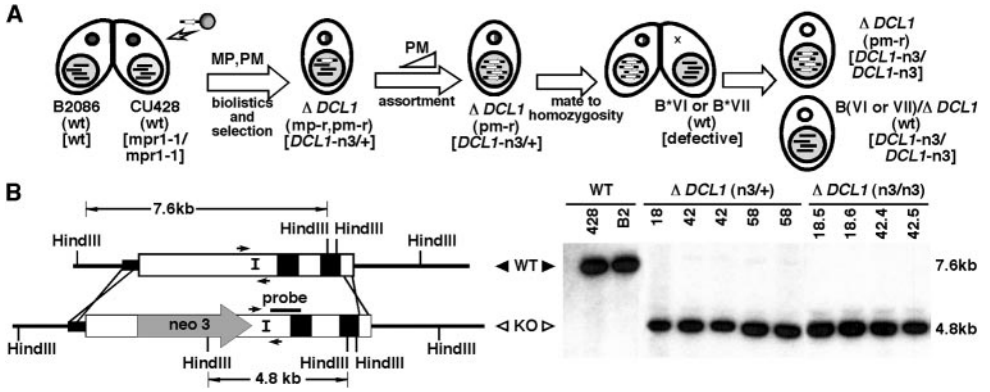

FIG. 2. Germ line knockout of *DCL1*. (A) Knockout strategy. Biolistic transformation was employed to introduce the *DCL1-neo3* (n3) knockout construct into wild-type (wt) strains, and transformant progeny were selected in PM and subsequently in 6-methyl purine (MP) and then assorted to complete replacement in increasing concentrations of PM. The solid lines in the diagram indicate wild-type chromosomes; the lines with white arrows indicate knockout chromosomes. Transformants were converted to homozygosity by genomic exclusion crosses. Exconjugants were separated and assayed for the presence of the knockout construct. Strains homozygous for the construct in the micro- and macronucleus were used for phenotypic analyses, while those homozygous in the micronucleus and wild type in the macronucleus were transformed with the GFP-*DCL1* construct and used in localization studies. Names are given below each strain with the macronuclear phenotype in parentheses and the micronuclear genotype in brackets. pm-r, paromomycin resistant. mp-r, 6-methyl purine resistant. (B) Southern blot analysis was used to verify the genotype Δ*DCL1* strains. Total genomic DNA was isolated, digested with HindIII, and hybridized with the *DCL1* probe shown in the diagram to the left. The region replaced by the *neo3* cassette (shaded arrow) relative to the conserved RNase III domains (solid boxes) and the lone intron (I) is depicted. The wild-type (WT) (closed triangle) and knockout (KO) (open triangle) HindIII fragments are 7.6 kb and 4.8 kb, respectively. Genomic DNA was analyzed from the two original wild-type strains, five somatic Δ*DCL1* strains that are heterozygous in the micronucleus (*n3*/+), and four somatic *DCL1* knockouts that are homozygous in the micronucleus for Δ*DCL1* (*n3*/*n3*) and which were derived from the heterozygotes shown.

vegetative growth as four or more cells were visible in each drop of medium by 24 h after mixing, the majority of Δ*DCL1* cells were still paired at this time. Most Δ*DCL1* pairs eventually separated, but the exconjugates never divided. Our results clearly show that *DCL1* is essential for *Tetrahymena* to complete development and return to vegetative growth.

The observed properties of the Δ*DCL1* strains we created were not entirely congruent with recently reported growth and developmental phenotypes of Δ*DCL1* strains generated by Mochizuki and Gorovsky (42). Most notably, their *DCL1* mutant strains exhibited defects during micronuclear division, resulting in the loss of chromosomal DNA that we did not observe in our knockout lines. In addition, their Δ*DCL1* cells showed significant aberrations during meiosis and progressed through conjugation asynchronously. This asynchrony may simply be a consequence of the observed meiotic defects. Based on these phenotypes, those authors concluded that *DCL1* has distinct roles in micronuclear chromosome segregation, meiotic prophase, and macronuclear development that our study cannot fully support. Conflicting results between their study and ours are not due to the differences in genetic backgrounds, as both studies used the same laboratory strains, but are likely due to the different knockout constructs used (see Discussion).

Δ*DCL1* cells do not generate germ line-specific small RNAs and accumulate nongenic micronuclear transcripts. Disruption of genes (e.g., *PDD1* and *TWI1*) that fail to stabilize small RNAs that have been linked to developmentally programmed DNA rearrangements exhibits developmental arrests very similar to those we observed for Δ*DCL1* cells (12, 40). We therefore asked whether our mutant cell lines fail to generate this specific class of small RNAs. These 28- to 30-nt RNA species are easily visualized on ethidium bromide-stained polyacrylamide gels by 2 h after mixing of wild-type cells and persist throughout conjugation (Fig. 4A and B) (40). In contrast, these small RNAs were undetectable in RNA isolated from Δ*DCL1* mating pairs at any point during development, indicating that this Dicer-related protein is required for their generation. We did not observe a reduction in the small RNA accumulation at any stage of conjugation upon mating of two *DCR1* somatic knockout lines, suggesting that this other Dicer-related protein is unnecessary for their generation (J. A. Motl and D. L. Chalker, unpublished data). In Δ*DCL1* mating cells, a barely perceptible amount of 23- to 24-nt RNAs appeared at later time points (Fig. 4G). These may result from processing of dsRNAs by *DCR1* and/or *DCR2*. Whether these smaller RNAs occur in wild-type cells and play a role in development and/or DNA rearrangement will require further investigation.

Clearly, the bulk of development-specific small RNAs are not produced in cells lacking *DCL1*. To assess whether the generation of small RNAs homologous to specific germ line-limited sequences that undergo DNA rearrangement is also affected in these mutants, we transferred stained RNAs to nylon membranes and hybridized these with strand-specific probes to detect ones homologous to the well-characterized M deletion element. We have previously shown that the M element is bidirectionally transcribed during development of wild-type cells (11) and that its small RNAs accumulate during the first 3 to 4 h of conjugation before they decline to a low steady-state level (9) (Fig. 4C and D). Just as we did not observe the bulk of developmental small RNAs in mating Δ*DCL1* cells, we could not detect small RNAs with probes specific to either strand of the M deletion element. Thus, *DCL1* is required to generate the small RNAs that correspond

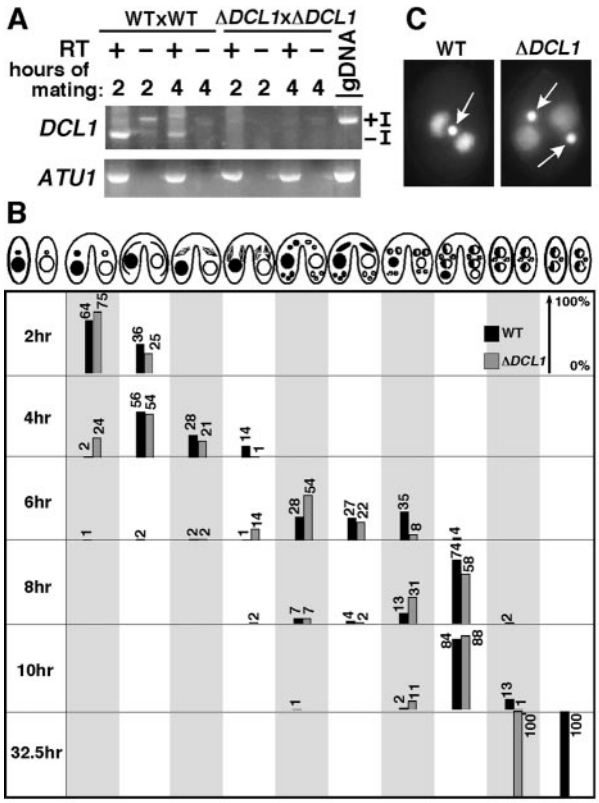

FIG. 3. Δ*DCL1* strains arrest late in conjugation. (A) RT-PCR was used to confirm that *DCL1* was not expressed in knockouts. Total RNA isolated at 2 and 4 h of mating was converted to cDNA to be used as a template for PCR amplification with *DCL1*-specific primers (Table 1), which are indicated as arrows in the knockout construct diagram (Fig. 2B). Identical reactions with *ATU* primers and wild-type (WT) genomic DNA (gDNA) served as positive controls for cDNA conversion and PCR amplification, respectively. Omission of reverse transcriptase (RT) controlled for the possibility of contaminating DNA in the reactions. (B) A diagram of the nuclear configuration diagnostic of individual stages is presented. The progression of wild-type (black bars) and Δ*DCL1* (gray bars) cells at individual time points after mixing was assessed by fluorescence microscopy of DAPI-staining cells. Numbers indicate the percentage of cell pairs at that stage of conjugation. (C) DAPI-stained cells showing the end point of development reached by wild-type and Δ*DCL1* cells at 32.5 h of conjugation. White arrows point to micronuclei.

to germ line-limited sequences that undergo DNA rearrangement.

If the nongenic transcripts of the M element are the precursors of these small RNAs, these larger transcripts should accumulate during conjugation of Δ*DCL1* cells. RNAs isolated from wild-type and Δ*DCL1* mating cells were fractionated on denaturing agarose gels and hybridized with M-element probes. In wild-type cells, transcripts homologous to both strands accumulate to relatively low levels, reaching their peak steady-state abundance approximately 6 h into conjugation (Fig. 4E and F) (11). On the other hand, M-element small RNA abundance peaks earlier, between 3 and 4 h of conjugation (Fig. 4C and D). We have argued that the large transcripts accumulate to their highest levels only after they cease being processed into small RNAs about 4 h into conjugation, when we see their levels begin to decline (9); however, this assumption requires that the large transcripts are indeed precursors of the small RNAs. In developing Δ*DCL1* cells, we observed that RNA species between ~200 and >1 kb corresponding to both M-element strands accumulated to significantly higher levels than in wild-type cells. The peak of accumulation was reached by 4 h into conjugation with lower steady-state levels persisting into the later time points. This peak in accumulation in the Δ*DCL1* cells is consistent with the interpretation that the larger transcripts, while still being synthesized, are processed by Dcl1p primarily during the first few hours of conjugation, when *DCL1* expression peaks. These data provide the first direct evidence that the larger bidirectional transcripts are precursors of the small RNAs that target DNA rearrangement of the M element and that Dcl1p is involved in this processing.

Dcl1p is localized in the micronucleus. The observation that M-element small RNAs cease to accumulate rather early in conjugation also corresponds to the drop in *DCL1* steady-state mRNA observed between 4 and 6 h after mixing (Fig. 1B). To further investigate the relationship between *DCL1* and small RNA generation, we examined the localization of Dcl1p by generating an amino-terminal fusion to GFP. This fusion protein was expressed ectopically under the cadmium-inducible MTT1 promoter (48) and maintained in *Tetrahymena* cells on a high-copy, rRNA gene-based replicating vector. GFP expressed alone from vector pIGF-1 produces bright green cells during either vegetative growth or conjugation, typically within 1 hour of cadmium addition (Fig. 5 and data not shown). The GFP-*DCL1* fusion construct was transformed into both wild-type strains and Δ*DCL1* lines to control for the possibility that localization was affected by the presence of endogenous Dcl1p. Induction of GFP-*DCL1* expression by cadmium addition to vegetatively growing cultures produced very little detectable GFP fluorescence and no specific localization, which is consistent with our inability to detect expression or observe a phenotype upon disruption in growing cells. This suggests that the fusion protein is either poorly translated or rapidly degraded compared to GFP alone. When we crossed GFP-DCL1-containing cells and induced expression at the beginning of conjugation, we observed distinct localization of the fusion protein to meiotic micronuclei in both wild-type cells and those lacking endogenous *DCL1* (Fig. 5). We typically detected GFP-*DCL1* in <10% of mating pairs, which may be indicative of variable expression from the MTT1 promoter in early conjugation or, more likely, that the protein has a short half-life, as GFP requires a period of time after translation to mature before it can fluoresce. We could first detect GFP-*DCL1* in micronuclei just prior to the onset of meiosis, but the fusion protein was most consistently visualized in late prophase, when the micronucleus forms an elongated "crescent" structure (47, 49). Comparison of the GFP localization to both the corresponding bright-field and DAPI-stained images reveals that Dcl1p is present in the nucleoplasm and appears to be primarily excluded from the DNA itself. In some cells, localization was somewhat punctate in crescent micronuclei for which the DNA was less condensed than the image shown, including specific accumulation in the narrow end of these structures. We detected little specific localization of the fusion protein after prophase, an observation that is congruent with the reduction in endogenous *DCL1* transcription and the cessation of small RNA generation. Taken together, our results allow us to con-

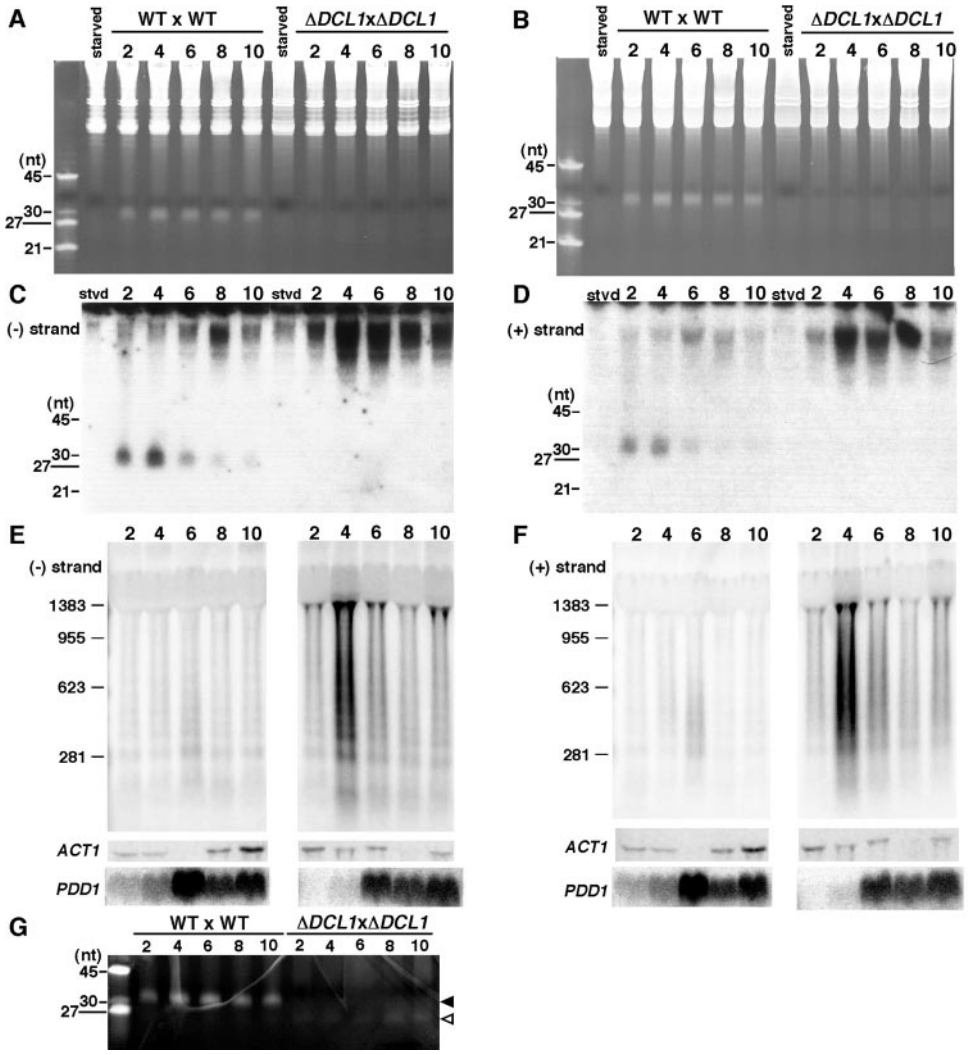

FIG. 4. Conjugating Δ*DCL1* strains exhibit loss of small RNA production and germ line transcript accumulation. RNA isolated at 2-h intervals from the start of conjugation was separated by electrophoresis on either 15% polyacrylamide–urea gels (A to D) or 1.2% agarose–formaldehyde gels (E and F), ethidium bromide stained (A and B) or transferred to membranes (C to F), and hybridized to plus-strand (+)- and minus-strand (−)-detecting M-element riboprobes as indicated. The migration of oligonucleotide (A to D) or RNA size standards (E and F) are indicated to the left of each panel. (A to D) RNA species of 28 to 30 nt (arrowhead) were observed throughout conjugation of wild-type (WT) cells but were undetected in starved (stvd) cells or Δ*DCL1* conjugating strains. (E and F) Northern blot analysis of Δ*DCLl* strains shows an accumulation of M-element bidirectional transcripts. Each filter was rehybridized with *ACT1* and *PDD1* probes for comparison of loading between samples and is shown below the corresponding panel. (G) Stained polyacrylamide gel of RNA isolated from wild-type or Δ*DCL1* cells that reveals smaller species of short RNAs (open arrowhead) migrating below the position of the abundant ~28-nt species (solid arrowhead).

clude that developmental small RNAs are generated by Dcl1p in the micronucleus.

Δ*DCL1* cells fail to eliminate germ line-limited sequences from developing macronuclei. As the transcription of germ line-limited sequences and the generation of small RNAs have been linked to *Tetrahymena* genome rearrangement, the failure of Δ*DCL1* cells to complete conjugation is likely due to a failure in this process. To examine this possibility, we isolated total genomic DNA from populations of wild-type and Δ*DCL1* cells well after the normal completion of macronuclear development (24 to 32 h) and examined the state of rearrangement of several loci by Southern blot analysis (Fig. 6). The 10-kbp genomic region of micronuclear chromosome 4 centered around the M deletion element contains two other germ line-limited sequences, designated the L (left) and R (right) elements (1) (Fig. 6A). Postconjugative wild-type cells had completely eliminated all three germ line-limited DNAs from newly formed somatic macronuclei as the ratio of rearranged to unrearranged chromosomes approached the ratio of macronuclear DNA to micronuclear DNA (15:1 to 20:1) typical for vegetative *Tetrahymena* (Fig. 6B). This was also observed for the germ line-limited sequence located upstream of the *Tetrahymena* calmodulin (CaM) gene (Fig. 6A and C) (29). In contrast, the chromosomes of postconjugative Δ*DCL1* cells retained the four germ line-limited sequences that are normally eliminated from the M-element genomic region and the CaM locus (Fig. 6B and C). The copies of the rearranged forms are likely derived from the 10 to 20% of unmated cells in the

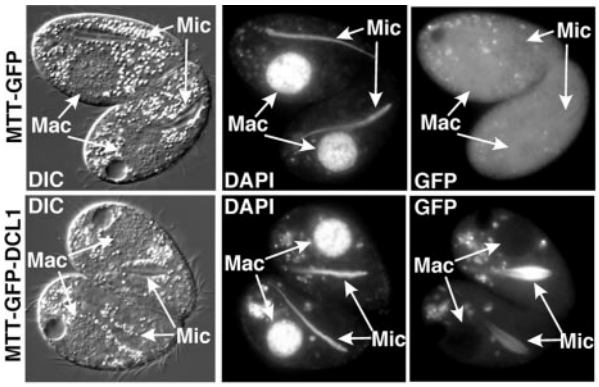

FIG. 5. The *DCL1* protein is localized to meiotic micronuclei. *Tetrahymena* transformed with pIGF-1, which contains GFP only (top panels) or a GFP-*DCL1* construct (bottom panels) was mated to nontransformed wild-type or Δ*DCL1* cells, and expression of the fusion protein was induced by the addition of $CdCl_2$ upon mixing of cells. Differential interference contrast (DIC) light microscopy of single pairs is displayed adjacent to fluorescence imaging of DAPI-stained DNA with and the localization of GFP or the GFP-*DCL1* fusion protein. The *DCL1* protein is observed exclusively in the extrachromosomal space in the elongated, meiotic (prophase) micronuclei (labeled as Mic). The location of the macronucleus (Mac) is also indicated. The mating partner with the brighter GFP fluorescence signal is likely the transformant expressing the GFP fusion that typically shows greater fluorescence despite extensive cytoplasmic exchange within the pair. Background fluorescence apparent in vacuoles is common in DAPI and GFP fluorescence in live *Tetrahymena* and accounts for the cytoplasmic signal observed.

population, and these appear overrepresented due to the polyploidy of the parental macronuclei and the apparent underamplification of developing macronuclei.

To further investigate the extent of failed DNA rearrangement, we examined the fate of the repetitive, germ line-limited sequence represented in clone Tt2512 (54). This >7-kbp sequence is present in the micronucleus at an estimated 50 to 100 loci and is entirely eliminated from the somatic macronucleus. Comparison of the level of hybridization of total genomic DNA from postconjugation wild-type and Δ*DCL1* cells revealed extensive retention of this sequence within the DNA isolated from the mutant strains (Fig. 6D and E). As the Tt2512 probe used hybridized exclusively to germ line-limited sequences, the observation that the majority of hybridizing fragments were much more abundant (quantified as 12- to 15-fold for the two strongest-hybridizing fragments) in the DNA of the mutant cell populations indicates that this repetitive sequence remained within the developing macronuclear genome at most or all its loci. Therefore, for each IES examined, we observed extensive failure of germ line DNA elimination, which demonstrates that Dcl1p is required for *Tetrahymena* genome rearrangements.

We also assessed the occurrence of chromosomal breakage in our *DCL1* mutants (Fig. 7). A membrane containing fractionated EcoRI-digested genomic DNA from postconjugative cells was hybridized with a radiolabeled probe that detected the left end of macronuclear chromosomal scaffold CH445662 (GenBank accession number gi62422284). In DNA from wild-type cells, the predominant hybridizing fragment was a 2.5-kbp species (Fig. 7), which is the size expected after chromosome breakage and addition of 250 to 300 bp of telomeric repeats. This species was absent in DNA recovered from the Δ*DLC1* mating cell population; but instead, the 10.5-kbp micronucleus-specific fragment was in higher abundance relative to the same fragment in wild-type cells. A less abundant population of fragments whose average size was ~2.6 kbp was observed in equal abundance in both populations. We interpret this by suggesting that the smaller, abundant fragments in wild-type cells are the result of new chromosome breakage and new telomere addition, while the majority of the larger fragments are derived from the macronuclei of the remaining unmated cells in the population that on average had longer telomeres. Thus, it appears that chromosome breakage is also perturbed in these *DCL1*-deficient cells.

Histone H3K9 methylation occurs, but is not targeted, in the absence of small RNAs. The chromatin associated with germ line-limited sequences is specifically methylated on lysine 9 of histone H3 prior to DNA rearrangement. Mutant cells lacking the chromodomain-containing protein Pdd1p or the Argonaute homologue Twi1p fail to establish this chromatin mark and eliminate germ line-limited DNA sequences (12, 34, 40, 50). This has led to the model that developmental small RNAs target this chromatin modification specifically to DNA segments that are eliminated from developing macronuclei (see reference 43). We expected that the disruption of *DCL1* that results in failure to generate the small RNAs would also abolish the establishment of the H3K9-methylated chromatin in developing macronuclei. Much to our surprise, when we examined total histone H3K9me2 on Western blots (Fig. 8A), we detected very little change in the overall modification of chromatin in Δ*DCL1* mating cells relative to wild-type cells, whereas our control using Δ*TWI1* cells showed no detectable H3K9me2 as previously reported (34). Similarly, after staining fixed conjugating cells with anti-H3K9me2 antibodies, little difference in the amounts of immunofluorescence was observed between wild-type and Δ*DCL1* cells (data not shown). Therefore, the generation of specific, small RNAs is not required for the establishment of this chromatin modification.

The fact that H3K9 methylation still occurred in our knockouts in the absence of the *DCL1*-generated small RNAs provided us the opportunity to ask whether these RNAs target this modification to specific loci. In wild-type cells, immunoprecipitation of conjugating cell chromatin with anti-H3K9me2 antibodies preferentially recovers germ line-limited sequences as demonstrated by a four- to fivefold enrichment of the adjacent M and R deletion elements but not the macronucleus-retained region between these IESs (Fig. 8B) (50). We did not observe enrichment of these same sequences in a chromatin immunoprecipitation assay of conjugating Δ*DCL1* cells. These data, along with our observation that these cells fail to eliminate numerous germ line-limited sequences, including the two examined here, provide convincing evidence that small RNAs direct this chromatin modification to the proper loci.

DISCUSSION

Distinct roles for Dicer-related proteins in growth and development. Three Dicer-related proteins encoded within the genome of *Tetrahymena thermophila* are each expressed at

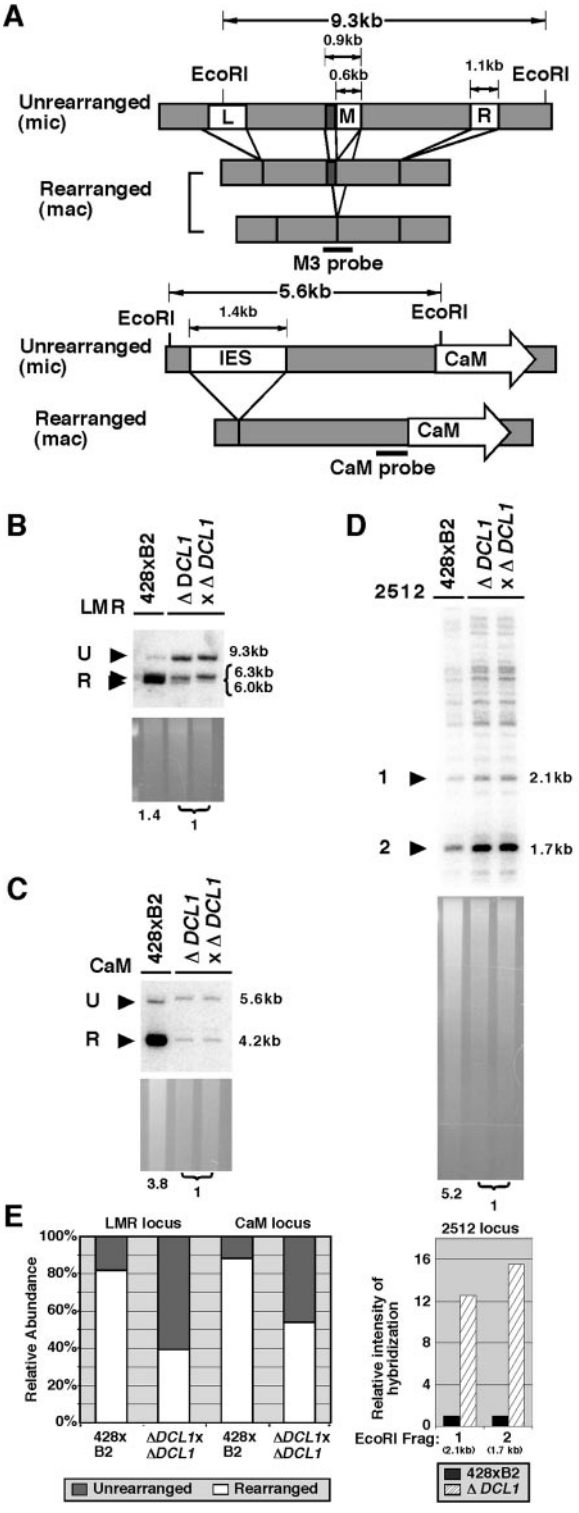

FIG. 6. *DCL1* knockouts fail to excise micronucleus-limited DNA. (A) Diagram of the micronuclear (mic) and macronuclear ¯L/M/R and CaM loci. IESs are indicated as open boxes, and macronucleus-destined sequences are indicated as shaded boxes. The L/M/R locus contains three IESs named the L (left), M (middle), and R (right) deletion elements. The M element has two alternative, leftward deletion boundaries that generate two rearranged forms of this loci at nearly equally frequencies. The genomic region upstream of the CaM gene contains a 1.4-kbp IES. The locations of the M3 and CaM probes used in Southern blot hybridization are shown (10). (B to D) Southern blot hybridization of DNA from postconjugative wild-type and Δ*DCL1* cells was used to assess IES rearrangement efficiency. For each blot, EcoRI-digested genomic DNA was fractionated, and specific loci were detected with (B) M3-, (C) CaM-, or (D) Tt2512-radiolabeled probes. The stained gel prior to blotting is shown for comparison of loading. Membranes were stripped and probed with the *ATU1* probe (not shown) to measure relative quantities of DNA loaded in each lane, which are reported at the bottom of each lane, with the Δ*DCL1* lanes set to 1 for ease of comparison. (E) Quantification of the rearranged (R) and unrearranged (U) forms in wild-type cells compared to Δ*DCL1* cells for the L/M/R and CaM loci and relative hybridization intensities (adjusted to *ATU1* hybridization) of EcoRI fragment (Frag) 1 (2.1 kb) and fragment 2 (1.7 kb) in the Tt2512 region in wild-type compared to *DCL1* knockout cells. The measured Tt2512 hybridization for wild-type cells was arbitrarily set to 1.

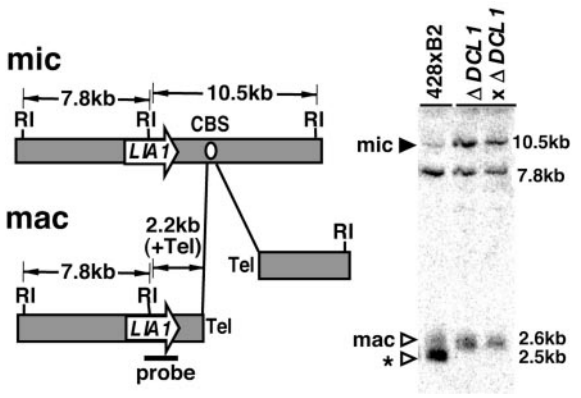

FIG. 7. Chromosome breakage does not occur in *DCL1* knockouts. The diagram shows the left end of macronuclear chromosomal scaffold CH445662, which contains the LIA1 gene within 2.5 kbp from the telomere (Tel), and the deduced ~18-kbp region of the micronuclear (mic) chromosome from which it is derived. The predicted location of the chromosomal breakage sequence (CBS) (white oval) is depicted as well as the relevant EcoRI (RI) restriction sites used for the Southern blot analysis of genomic DNA from postconjugative wild-type and Δ*DCL1* cells used to assess chromosome breakage. The probe spans the central EcoRI site and detects a 7.8-kbp fragment common to both nuclei, which can be used to compare amounts of DNA loaded between each lane, and either the ~10.5-kbp micronucleus-specific fragment (solid arrowhead) or a 2.5- to 2.6-kbp macronucleus-specific fragment (2.2 kbp of unique sequence plus 300 to 400 bp of telomeric DNA) (open arrowheads). The shorter macronuclear fragments marked by the asterisk appear only in wild-type samples and are likely derived from new chromosomal breakage and telomere addition in developing macronuclei, while the larger fragments are presumed to be derived from the macronuclei of unmated cells with, on average, longer telomeres.

different levels and stages of this ciliate's life cycle (Fig. 1). *DCR1* and *DCR2* genes are expressed in vegetative cells, and our inability to completely knock out *DCR2* suggests that it is essential for growth. Neither *DCR1* nor *DCL1* is required for vegetative growth, as we generated complete somatic knockouts of these genes. However, we found that *DCL1*, which is expressed at high levels only during conjugation, is required to complete development. *DCR1* somatic knockouts complete development normally, but as we disrupted only the somatic copies of this gene and not those in the silent, germ line micronucleus, we cannot rule out that it has a role in late stages of conjugation after zygotic expression begins and the wild-

type germ line copies would be expressed. Similar findings were recently reported by Mochizuki and Gorovsky (42). It is clear that these three putative RNase III enzymes have distinct, nonredundant functions in growth and/or development.

The extensive genome rearrangements that occur during *Tetrahymena* development are guided by an RNAi-like mechanism (reviewed in reference 43) which overall exhibits remarkable similarities to the establishment of heterochromatin in other eukaryotes (reviewed in reference 23). In addition to finding that Δ*DCL1* cells arrest late in development, we observed that Δ*DCL1* cells do not generate abundant developmental small RNAs but instead accumulate germ line-limited transcripts homologous to eliminated sequences (Fig. 4). This provides direct evidence that the bidirectional transcripts synthesized during meiotic prophase (11, 39, 49) are the precursors of these abundant RNA species. Furthermore, postconjugative Δ*DCL1* cells failed to eliminate all germ line-limited sequences assayed, providing proof that these RNAs guide genome rearrangement. Δ*DCL1* cells also failed in chromosomal breakage, but we have less evidence to argue that this is a direct effect and not an indirect result of the developmental arrest observed that could occur prior to completion of this process.

The phenotypes of our Δ*DCL1* cells had many similarities but also some marked differences from those described in the *DCL1* study published previously by Mochizuki and Gorovsky (42). One obvious disparate phenotype is their reported defects in micronuclear division during vegetative growth that we do not observe in our Δ*DCL1* cells. We have difficulty attributing this phenotype to the loss of *DCL1* because we cannot detect its expression in vegetative cells using RT-PCR conditions that would have detected even one transcript per cell (Fig. 1C). Nevertheless, we must note that our Δ*DCL1* cells retained additional coding sequence, compared to the cells of the other study, that could potentially rescue some *DCL1* function. To eliminate the possibility of rescue of some *DCL1* function due to undetected expression of a C-terminal polypeptide that retained catalytic activity, we generated new *DCL1* macronuclear knockout lines that removed an additional 464 codons including most of both RNase III domains. These Δ*DCL1* strains exhibited the same developmental arrest phenotype as our original knockout lines, as the majority of cells died with two micronuclei and two developing macronuclei (data not shown) rather than the asynchronous arrest observed by Mochizuki and Gorovsky. Our knockout strains also retained the 189 amino-terminal codons that could theoretically rescue some *DCL1* function, as we did not remove the promoter and can detect transcription of this region in conjugating cells by RT-PCR. However, any rescue must be independent of the RNase activity of this protein. The phenotypes we report above are fully consistent with an exclusive and critical role for Dcl1p in macronuclear development. Nevertheless, if expression of a partial polypeptide within our Δ*DCL1* lines rescues secondary roles of this protein in micronuclear maintenance, the *DCL1* allele that we have created has allowed us to separate the distinct roles of this Dicer-related protein.

An alternative explanation is that the micronucleus-associated phenotypes of the Δ*DCL1* strains reported by Mochizuki and Gorovsky are due to perturbation of another gene in addition to disruption of *DCL1*. One obvious candidate would be the predicted open reading frame immediately upstream of *DCL1*. The last predicted codon of this open reading frame is just under 1 kbp from the *DCL1* start methionine. Disruption of this upstream coding sequence, along with *DCL1*, resulted in suboptimal growth with noticeable cell death, particularly during stationary phase and starvation (D. L. Chalker, unpublished); thus, partial loss of function of this upstream gene could conceivably interfere with proper micronuclear segregation, as was observed previously (42). These double-knockout strains were unable to efficiently initiate conjugation due to starvation defects that inhibited our ability to examine meiotic phenotypes. However, the sequence of this predicted gene was not altered and remains transcribed in their strains (K. Mochizuki, personal communication), so an obvious perturbation is not evident. All tests aimed to resolve the differences between the different *DCL1* mutant strains have proved inconclusive.

While *DCL1* is essential for the accumulation of develop-

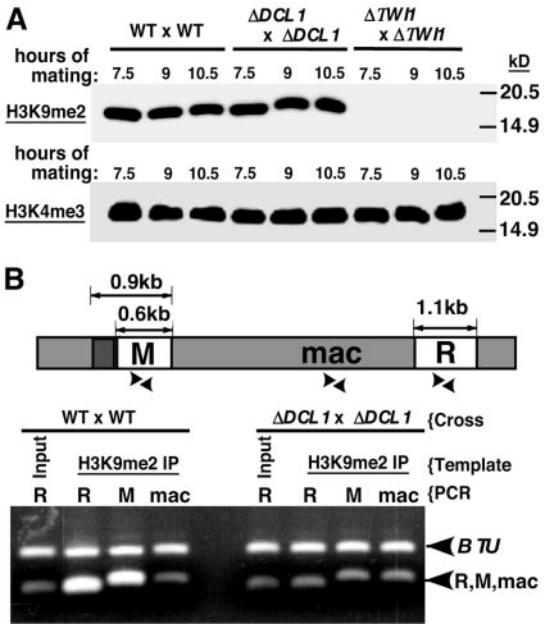

FIG. 8. *DCL1* is not required for H3K9 methylation. (A) Total cell protein extracts isolated from conjugating wild-type (WT), Δ*DCL1*, or Δ*TWI1* cells at the indicated times after mixing were fractionated by SDS-polyacrylamide gel electrophoresis for Western blot analysis. The overall level of modified histone H3 was assessed with antibodies detecting histone H3K9me2 (dimethyl) (top) or histone H3K4me3 (trimethyl) (bottom). The positions of protein molecular mass standards (in kilodaltons [kD]) are given on the right. (B) Representative PCR results after chromatin immunoprecipitation with anti-H3K9me2-specific antibodies from 9-h mating *Tetrahymena* cells. PCR products of specific amplified fragments of the R or M element or the intervening macronucleus-retained sequence were separated by 1.6% agarose gel electrophoresis and stained with ethidium bromide. The locations of amplification primers are shown in the diagram of the analyzed genomic region as arrowheads. Input designates that the DNA template was recovered from chromatin preparations prior to immunoprecipitation (only amplification of input using R-element primers is shown; the upper band corresponds to amplification of a quantification control from the *BTU1* locus, and the lower band corresponds to the IES or macronucleus-retained locus [indicated above each lane]).

mental small RNAs, we cannot discount the possibility that its protein participates in an initial step of processing and that *DCR1* and/or *DCR2* may also be involved in additional RNA processing. Dcl1p could play a role similar to that of Drosha, an RNase III enzyme also lacking a helicase domain that is required for processing primary miRNA transcripts but not the final processing steps that generate mature miRNAs (16, 32). We think this is less likely as *DCR1* and *DCR2* are expressed at relatively low levels early in conjugation and *DCR1* is dispensable for production of these small RNAs (J. A. Motl and D. L. Chalker, unpublished). Further investigation into the role of these other Dicer-related proteins is required to determine their roles, if any, in *Tetrahymena* DNA rearrangement.

Small RNA processing is not required for chromatin modification. Disruption of *DCL1* abolished small RNA production and DNA rearrangement but was not sufficient to eliminate H3K9me2 establishment (Fig. 8). In contrast, Mochizuki and Gorovsky (42) did not detect this chromatin modification occurring in their *DCL1* knockout lines, although it should be noted that their cells exhibited severe developmental abnormalities with <5% even progressing to form new macronuclei. While this subset of cells showed normal localization of Pdd1p, its localization is independent of this chromatin modification (34) and cannot be taken as an indicator that these cells may not have other defects that interfered with this modification. As our Δ*DCL1* cells did not exhibit these early development phenotypes, we were able to more thoroughly examine the knockout phenotype throughout mating, and we observed H3K9 methylation in the absence of small RNAs. However, this modification was no longer enriched on germ line-limited IESs, an observation that convincingly demonstrates that DCL1-generated small RNAs guide H3K9 methylation to the homologous locus.

It is intriguing to us that H3K9me2 chromatin is established in the absence of *DCL1*. This modification was not detected in strains lacking the Argonaute protein Twi1p (Fig. 8; 34) or the chromodomain-containing Pdd1p (50). This difference may indicate that both of these proteins are part of the effector complex that uses small RNAs to target this histone modification to specific loci. Loss of either protein may disrupt the complex and thereby abolish all H3K9 methylation. Both Pdd1p and Twi1p are initially localized in the cytoplasm before relocating to the developing macronucleus, an observation that is consistent with a putative association between them (36, 40). In contrast, Dcl1p is localized to the micronucleus and does not appear to relocalize to the developing nuclei where this modification occurs. In the absence of the abundant small RNAs, this H3K9 methylation complex appears to be directed to chromatin indiscriminately, modifying sequences other than germ line-limited DNA, or to be targeted to some specific regions by an unknown parallel path. In *Schizosaccharomyces pombe*, ATF/CREB proteins can target this modification in the absence of RNAi proteins (28), and a similar pathway may exist in *Tetrahymena*, although it is insufficient to replace all *DCL1* function.

Compartmentalization of the steps in DNA rearrangement. We have previously argued that the temporal separation of small RNA biogenesis early in conjugation from targeting later in development is instrumental to the proper regulation of this process (9). Mechanistically, the localization of *DCL1* within the micronucleus provides an important compartmentalization of this early RNA processing step in DNA rearrangement. To ensure that only the germ line-limited sequences are excised by this irreversible process, *Tetrahymena* cells confine the generation of the targeting small RNAs to the germ line nucleus. Initially, small RNAs homologous to somatic-retained sequences may also be produced, but a proofreading mechanism is postulated to check this initial pool for homology against the sequences within the parental macronucleus (40). This idea is evinced by the failure to eliminate sequences that are usually efficiently excised in the event that the homologous sequence is found within the parental macronucleus (10). This proofreading mechanism is likely mediated by the Twi1p-containing complexes that pick up small RNAs in the cytoplasm and transport them to the parental macronucleus (40, 41). Complexes that interact with a homologous sequence within this nucleus must be inactivated or disassembled and cannot target subsequent DNA rearrangement. We have suggested that these RNA-protein complexes actually interact with homologous transcripts rather than the DNA itself, given that introduced sequences previously shown to block elimination are bidirectionally transcribed (9). The failure of these bidirectional transcripts that are synthesized in the parental macronucleus to be processed into small RNAs further supports a compartmentalization Dicer function (9).

It is unclear whether meiotic micronuclear transcription is concentrated on germ line-limited sequences or extends over most of the genome; however, the *DCL1*-dependent small RNAs are enriched in germ line-limited sequences as early as 2 h into conjugation, which is indicative of some selectivity in this transcription (41). The germ line-limited M and R deletion elements are developmentally transcribed even when placed into the somatic macronucleus, which leads us to argue that sequences that normally undergo DNA rearrangement can be recognized and thus can be preferentially transcribed (9, 11). The increase in levels of nongenic, micronuclear transcripts detected in Δ*DCL1* cells (Fig. 4E and F) is similar to observations made in Dicer-deficient *S. pombe* and DT-40 human-chicken hybrid cells that accumulate transcripts corresponding to the outer centromere repeats and α-satellite sequences, respectively (18, 51). These rather different repetitive sequences all produce noncoding RNAs and exhibit RNAi-directed heterochromatin assembly. These shared properties may be suggestive of a conserved mechanism underlying these rather unconventional transcriptional phenomena. A novel RNA polymerase, polymerase IV, recently discovered in plants, has been shown to be required for RNAi-mediated gene silencing and facultative heterochromatin assembly (26, 44). While polymerase IV may be plant specific, its existence suggests that RNAi-related nongenic transcription may have unique requirements. Further study of the specificity of *Tetrahymena* germ line transcription is sure to shed light on this process.

ACKNOWLEDGMENTS

This work was supported by National Science Foundation research grant MCB-0131421 and by National Institutes of Health research grant GM069593 to D.L.C.

We thank Washington University Biology 3492 students (Eric Archer, Robert Cooper, Laura Ernst, Michael Evenson, Annabel Fu, Xiaoou Pan, and Andrew Schmerling) for technical assistance with the

project. We also thank Martin Gorovsky (University of Rochester) for providing plasmid pMNBL and K. Mochizuki (University of Rochester) for providing the Δ*TWI1* strains, sharing unpublished data, and comments on our manuscript. Preliminary *Tetrahymena* genome sequence data were obtained from The Institute for Genomic Research website (http://www.tigr.org).

REFERENCES

1. **Austerberry, C. F., C. D. Allis, and M. C. Yao.** 1984. Specific DNA rearrangements in synchronously developing nuclei of *Tetrahymena*. Proc. Natl. Acad. Sci. USA **81:**7383–7387.
2. **Ausubel, F. M., R. Brent, R. E. Kingston, D. D. Moore, J. G. Seidman, J. A. Smith, and K. Struhl (ed.).** 1990. Current protocols in molecular biology. John Wiley & Sons, New York, N.Y.
3. **Bernstein, E., A. A. Caudy, S. M. Hammond, and G. J. Hannon.** 2001. Role for a bidentate ribonuclease in the initiation step of RNA interference. Nature **409:**363–366.
4. **Bruns, P. J., and D. Cassidy-Hanley.** 2000. Biolistic transformation of macro- and micronuclei. Methods Cell Biol. **62:**501–512.
5. **Bruns, P. J., and D. Cassidy-Hanley.** 2000. Methods for genetic analysis. Methods Cell Biol. **62:**229–240.
6. **Carmell, M. A., and G. J. Hannon.** 2004. RNase III enzymes and the initiation of gene silencing. Nat. Struct. Mol. Biol. **11:**214–218.
7. **Cassidy-Hanley, D., J. Bowen, J. H. Lee, E. Cole, L. A. VerPlank, J. Gaertig, M. A. Gorovsky, and P. J. Bruns.** 1997. Germline and somatic transformation of mating *Tetrahymena thermophila* by particle bombardment. Genetics **146:**135–147.
8. **Chalker, D., A. La Terza, A. Wilson, C. Kroenke, and M. Yao.** 1999. Flanking regulatory sequences of the *Tetrahymena* R deletion element determine the boundaries of DNA rearrangement. Mol. Cell. Biol. **19:**5631–5641.
9. **Chalker, D. L., P. Fuller, and M. C. Yao.** 2005. Communication between parental and developing genomes during *Tetrahymena* nuclear differentiation is likely mediated by homologous RNAs. Genetics **169:**149–160.
10. **Chalker, D. L., and M.-C. Yao.** 1996. Non-Mendelian, heritable blocks to DNA rearrangement are induced by loading the somatic nucleus of *Tetrahymena thermophila* with germ line-limited DNA. Mol. Cell. Biol. **16:**3658–3667.
11. **Chalker, D. L., and M. C. Yao.** 2001. Nongenic, bidirectional transcription precedes and may promote developmental DNA deletion in *Tetrahymena thermophila*. Genes Dev. **15:**1287–1298.
12. **Coyne, R. S., M. A. Nikiforov, J. F. Smothers, C. D. Allis, and M. C. Yao.** 1999. Parental expression of the chromodomain protein Pdd1p is required for completion of programmed DNA elimination and nuclear differentiation. Mol. Cell **4:**865–872.
13. **Duharcourt, S., A. Butler, and E. Meyer.** 1995. Epigenetic self-regulation of developmental excision of an internal eliminated sequence in *Paramecium tetraurelia*. Genes Dev. **9:**2065–2077.
14. **Duharcourt, S., A. Keller, and E. Meyer.** 1998. Homology-dependent maternal inhibition of developmental excision of internal eliminated sequences in *Paramecium tetraurelia*. Mol. Cell. Biol. **18:**7075–7085.
15. **Fan, Q., R. Sweeney, and M.-C. Yao.** 1999. Creation and use of antisense ribosomes in *Tetrahymena thermophila*, p. 533–547. *In* D. J. Asai and J. D. Forney (ed.), *Tetrahymena thermophila*, vol. 62. Academic Press, New York, N.Y.
16. **Filippov, V., V. Solovyev, M. Filippova, and S. S. Gill.** 2000. A novel type of RNase III family proteins in eukaryotes. Gene **245:**213–221.
17. **Fillingham, J. S., D. Bruno, and R. E. Pearlman.** 2001. Cis-acting requirements in flanking DNA for the programmed elimination of mse2.9: a common mechanism for deletion of internal eliminated sequences from the developing macronucleus of *Tetrahymena thermophila*. Nucleic Acids Res. **29:**488–498.
18. **Fukagawa, T., M. Nogami, M. Yoshikawa, M. Ikeno, T. Okazaki, Y. Takami, T. Nakayama, and M. Oshimura.** 2004. Dicer is essential for formation of the heterochromatin structure in vertebrate cells. Nat. Cell Biol. **6:**784–791.
19. **Gaertig, J., L. Gu, B. Hai, and M. A. Gorovsky.** 1994. High frequency vector-mediated transformation and gene replacement in *Tetrahymena*. Nucleic Acids Res. **22:**5391–5398.
20. **Garnier, O., V. Serrano, S. Duharcourt, and E. Meyer.** 2004. RNA-mediated programming of developmental genome rearrangements in *Paramecium tetraurelia*. Mol. Cell. Biol. **24:**7370–7379.
21. **Godiska, R., C. James, and M. C. Yao.** 1993. A distant 10-bp sequence specifies the boundaries of a programmed DNA deletion in *Tetrahymena*. Genes Dev. **7:**2357–2365.
22. **Godiska, R., and M. C. Yao.** 1990. A programmed site-specific DNA rearrangement in *Tetrahymena thermophila* requires flanking polypurine tracts. Cell **61:**1237–1246.
23. **Grewal, S. I., and J. C. Rice.** 2004. Regulation of heterochromatin by histone methylation and small RNAs. Curr. Opin. Cell Biol. **16:**230–238.
24. **Grishok, A., A. E. Pasquinelli, D. Conte, N. Li, S. Parrish, I. Ha, D. L. Baillie, A. Fire, G. Ruvkun, and C. C. Mello.** 2001. Genes and mechanisms related to RNA interference regulate expression of the small temporal RNAs that control *C. elegans* developmental timing. Cell **106:**23–34.
25. **Hannon, G. J.** 2002. RNA interference. Nature **418:**244–251.
26. **Herr, A. J., M. B. Jensen, T. Dalmay, and D. C. Baulcombe.** 2005. RNA polymerase IV directs silencing of endogenous DNA. Science **308:**118–120.
27. **Hutvagner, G., J. McLachlan, A. E. Pasquinelli, E. Balint, T. Tuschl, and P. D. Zamore.** 2001. A cellular function for the RNA-interference enzyme Dicer in the maturation of the let-7 small temporal RNA. Science **293:**834–838.
28. **Jia, S., K. Noma, and S. I. Grewal.** 2004. RNAi-independent heterochromatin nucleation by the stress-activated ATF/CREB family proteins. Science **304:**1971–1976.
29. **Katoh, M., M. Hirono, T. Takemasa, M. Kimura, and Y. Watanabe.** 1993. A micronucleus-specific sequence exists in the 5′-upstream region of calmodulin gene in *Tetrahymena thermophila*. Nucleic Acids Res. **21:**2409–2414.
30. **Ketting, R. F., S. E. Fischer, E. Bernstein, T. Sijen, G. J. Hannon, and R. H. Plasterk.** 2001. Dicer functions in RNA interference and in synthesis of small RNA involved in developmental timing in *C. elegans*. Genes Dev. **15:**2654–2659.
31. **Kurihara, Y., and Y. Watanabe.** 2004. Arabidopsis micro-RNA biogenesis through Dicer-like 1 protein functions. Proc. Natl. Acad. Sci. USA **101:**12753–12758.
32. **Lee, Y., C. Ahn, J. Han, H. Choi, J. Kim, J. Yim, J. Lee, P. Provost, O. Radmark, S. Kim, and V. N. Kim.** 2003. The nuclear RNase III Drosha initiates microRNA processing. Nature **425:**415–419.
33. **Lee, Y. S., K. Nakahara, J. W. Pham, K. Kim, Z. He, E. J. Sontheimer, and R. W. Carthew.** 2004. Distinct roles for Drosophila Dicer-1 and Dicer-2 in the siRNA/miRNA silencing pathways. Cell **117:**69–81.
34. **Liu, Y., K. Mochizuki, and M. A. Gorovsky.** 2004. Histone H3 lysine 9 methylation is required for DNA elimination in developing macronuclei in *Tetrahymena*. Proc. Natl. Acad. Sci. USA **101:**1679–1684.
35. **Liu, Y., X. Song, M. A. Gorovsky, and K. M. Karrer.** 2005. Elimination of foreign DNA during somatic differentiation in *Tetrahymena thermophila* shows position effect and is dosage dependent. Eukaryot. Cell **4:**421–431.
36. **Madireddi, M. T., R. S. Coyne, J. F. Smothers, K. M. Mickey, M.-C. Yao, and C. D. Allis.** 1996. Pdd1p, a novel chromodomain-containing protein, links heterochromatin assembly and DNA elimination in *Tetrahymena*. Cell **87:**75–84.
37. **Madireddi, M. T., M. Davis, and D. Allis.** 1994. Identification of a novel polypeptide involved in the formation of DNA-containing vesicles during macronuclear development in *Tetrahymena*. Dev. Biol. **165:**418–431.
38. **Martindale, D. W., C. D. Allis, and P. Bruns.** 1982. Conjugation in *Tetrahymena thermophila*: a temporal analysis of cytological stages. Exp. Cell Res. **140:**227–236.
39. **Martindale, D. W., C. D. Allis, and P. J. Bruns.** 1985. RNA and protein synthesis during meiotic prophase in *Tetrahymena thermophila*. J. Protozool. **32:**644–649.
40. **Mochizuki, K., N. A. Fine, T. Fujisawa, and M. A. Gorovsky.** 2002. Analysis of a piwi-related gene implicates small RNAs in genome rearrangement in *Tetrahymena*. Cell **110:**689–699.
41. **Mochizuki, K., and M. A. Gorovsky.** 2004. Conjugation-specific small RNAs in *Tetrahymena* have predicted properties of scan (scn) RNAs involved in genome rearrangement. Genes Dev. **18:**2068–2073.
42. **Mochizuki, K., and M. A. Gorovsky.** 2005. A Dicer-like protein in *Tetrahymena* has distinct functions in genome rearrangement, chromosome segregation, and meiotic prophase. Genes Dev. **19:**77–89.
43. **Mochizuki, K., and M. A. Gorovsky.** 2004. Small RNAs in genome rearrangement in *Tetrahymena*. Curr. Opin. Genet. Dev. **14:**181–187.
44. **Onodera, Y., J. R. Haag, T. Ream, P. C. Nunes, O. Pontes, and C. S. Pikaard.** 2005. Plant nuclear RNA polymerase IV mediates siRNA and DNA methylation-dependent heterochromatin formation. Cell **120:**613–622.

44a. **Orias, E., E. P. Hamilton, and J. D. Orias.** 1999. *Tetrahymena* as a laboratory organism: useful strains, cell culture, and cell line maintenance. Methods Cell Biol. **62:**189–211.

45. **Patil, N., and K. Karrer.** 2000. A developmentally regulated deletion element with long terminal repeats has cis-acting sequences in the flanking DNA. Nucleic Acids Res. **28:**1465–1472.
46. **Prescott, D. M.** 1994. The DNA of ciliated protozoa. Microbiol. Rev. **58:**233–267.
47. **Ray, C. J.** 1956. Meiosis and nuclear behavior in *Tetrahymena pyriformis*. J. Protozool. **3:**88–96.
48. **Shang, Y., X. Song, J. Bowen, R. Corstanje, Y. Gao, J. Gaertig, and M. A. Gorovsky.** 2002. A robust inducible-repressible promoter greatly facilitates gene knockouts, conditional expression, and overexpression of homologous and heterologous genes in *Tetrahymena thermophila*. Proc. Natl. Acad. Sci. USA **99:**3734–3739.
49. **Sugai, T., and K. Hiwatashi.** 1974. Cytological and autoradiographic studies of the micronucleus at meiotic prophase in *Tetrahymena pyriformis*. J. Protozool. **21:**542–548.

50. **Taverna, S. D., R. S. Coyne, and C. D. Allis.** 2002. Methylation of histone h3 at lysine 9 targets programmed DNA elimination in *Tetrahymena*. Cell **110:** 701–711.
51. **Volpe, T. A., C. Kidner, I. M. Hall, G. Teng, S. I. Grewal, and R. A. Martienssen.** 2002. Regulation of heterochromatic silencing and histone H3 lysine-9 methylation by RNAi. Science **297:**1833–1837.
52. **Wenkert, D., and C. D. Allis.** 1984. Timing of the appearance of macronuclear-specific histone variant hv1 and gene expression in developing new macronuclei of *Tetrahymena thermophila*. J. Cell Biol. **98:**2107–2117.
53. **Xie, Z., L. K. Johansen, A. M. Gustafson, K. D. Kasschau, A. D. Lellis, D. Zilberman, S. E. Jacobsen, and J. C. Carrington.** 2004. Genetic and functional diversification of small RNA pathways in plants. PLoS Biol. **2:**E104.
54. **Yao, M. C.** 1982. Elimination of specific DNA sequences from the somatic nucleus of the ciliate *Tetrahymena*. J. Cell Biol. **92:**783–789.
55. **Yao, M. C., S. Duharcourt, and D. L. Chalker.** 2002. Genome-wide rearrangements of DNA in ciliates, p. 730–758. *In* N. Craig, R. Craigie, M. Gellert, and A. Lambowitz (ed.), Mobile DNA II. Academic Press, New York, N.Y.
56. **Yao, M. C., P. Fuller, and X. Xi.** 2003. Programmed DNA deletion as an RNA-guided system of genome defense. Science **300:**1581–1584.